Dynamics Based Neural Encoding with Inter-Intra Region Connectivity

Mai Gamal
German University in Cairo
Egypt
mai.tharwat@guc.edu.eg

Mohamed Rashad
Ain Shams University
Egypt
mohamed.rashad@cis.asu.edu.eg

Eman Ehab
Nile University
Egypt
e.ehab@nu.edu.eg

Seif Eldawlatly
American University in Cairo
Egypt
seldawlatly@aucegypt.edu

Mennatullah Siam
University of British Columbia
Canada
mennatullah.siam@ubc.ca

ABSTRACT

Extensive literature has drawn comparisons between recordings of biological neurons in the brain and deep neural networks. This comparative analysis aims to advance and interpret deep neural networks and enhance our understanding of biological neural systems. However, previous works did not consider the time aspect and how the encoding of video and dynamics in deep networks relate to the biological neural systems within a large-scale comparison. Towards this end, we propose the first large-scale study focused on comparing video understanding models with respect to the visual cortex recordings using video stimuli. The study encompasses more than two million regression fits, examining image *vs.* video understanding, convolutional *vs.* transformer-based and fully *vs.* self-supervised models. Our study resulted in both, insights to help better understand deep video understanding models and a novel neural encoding scheme to better encode biological neural systems. We provide key insights on how video understanding models predict visual cortex responses; showing video understanding better than image understanding models, convolutional models are better in the early-mid visual cortical regions than transformer based ones except for multiscale transformers and that two-stream models are better than single stream. Furthermore, we propose a novel neural encoding scheme that is built on top of the best performing video understanding models, while incorporating inter-intra region connectivity across the visual cortex. Our neural encoding leverages the encoded dynamics from video stimuli, through utilizing two-stream networks and multiscale transformers, while taking connectivity priors into consideration. Our results show that merging both intra and inter-region connectivity priors increases the encoding performance over each one of them standalone or no connectivity priors. It also shows the necessity for encoding dynamics to fully benefit from such connectivity priors.

1 INTRODUCTION

There has been a recent increase in studies that compare how deep neural networks process input stimuli to the processing that occurs in the brain whether in humans Zhou et al. (2022); Conwell et al. (2021b); Schrimpf et al. (2018); Cichy et al. (2019; 2021), non-human primates, or rodents Conwell et al. (2021a); Schrimpf et al. (2018). The benefits of these studies are two-fold. First, such a comparison can be used to interpret and have a better understanding of black-box deep neural

networks and even provide inspirations on how to improve them. Second, it can provide a better understanding and encoding of biological neural systems. Towards achieving this, recent benchmarks have been released to improve the capabilities of machine learning models in neural encoding and comparing them to biological neural systems Schrimpf et al. (2018); Cichy et al. (2019; 2021); Gifford et al. (2023). The current established benchmark from The Mini-Algonauts Project 2021 Cichy et al. (2021), has provided neuro-imaging data for the brain responses from participants watching short video clips. A further extension of the aforementioned dataset Lahner et al. (2024) provided exhaustive analysis with additional cortical regions for the ventral and dorsal streams. It also provided empirical evidence that temporal information was captured in fMRI recordings of the visual cortex for participants watching video stimuli, through studying the effect of frame shuffling and analyzing the first and last second of these videos. The former showed that shuffling lead to degraded performance confirming that there are dynamics captured in the recorded fMRI, while the later showed that these fMRI recordings encode temporally distinct early and late video snapshots. These developments and benchmarks can enable neuroscientists to study how the brain understands dynamics (e.g., motion), which is critical to study in neural encoding.

Machine learning models have been investigated in encoding such neuro-imaging data Lahner (2022); Zhou et al. (2022); Lahner et al. (2024). However, these studies either focused on a small-scale comparison of few video understanding models or conducted their study on single image based models, neglecting the dynamics aspect. More importantly, previous studies did not conduct a systematic analysis of different model families. To address this gap, we propose the first large-scale comparative study of video understanding in neural encoding that encompasses more than two million regression fits (this refers to source models, their layers, target models, regions, and voxels count). Our study takes various properties into consideration where we study image *vs.* video understanding, convolutional *vs.* transformer based, single-stream *vs.* two-stream and fully supervised *vs.* self supervised ones. Furthermore, we not only study these video understanding models to encode cortical regions recordings, we also study them in a simulated setup where the target is another neural network, inspired by the single image understanding study Han et al. (2023). Our results show that video understanding models are better than image understanding ones in modelling the human visual cortex recordings. Specifically, two-stream convolutional models and multiscale transformers were the best ones. Interestingly, we are the first to demonstrate the effect of multiscale processing in transformers that improves its ability to capture low level cues (e.g. oriented gradients) consequently improving its performance in the early regions.

Finally, we devise a novel neural encoding mechanism that takes into account encoded dynamics and connectivity priors. Voxel connectivity started to get explored in neural encoding in few recent works Mell et al. (2021); Xiao et al. (2022). However, previous works used this approach in a limited scope in which they studied the connectivity between pairs of regions without considering the connectivity across all regions at once. They also did not consider the combined effect of the local connectivity within the same region (intra-region connectivity) and the global connectivity across the different regions (inter-region connectivity).

In summary, our contributions are three fold:

- We showcase the first large-scale study of deep video understanding models on two datasets for the human visual cortex where the models include convolutional *vs.* transformer-based, single *vs.* two stream and fully *vs.* self-supervised. Our study is comprehensive with more than 35 models from various families and more than two million regression fits, unlike the recent work Lahner et al. (2024) that showed only three models with limited types.

- We establish a simulated environment setup using image and video understanding models as the target and a real environment setup with the target model as the human visual cortex.

- We propose a novel fully integrated encoding model that takes into account intra and inter-region connectivity priors in the visual cortex with features extracted from pre-trained video understanding models. We also show that encoding dynamics is an important aspect to enable the full utilization of such connectivity priors.

2 RELATED WORK

Biological neural systems encoding. Brain encoding is concerned with mapping the input stimuli to the neural activations in the brain. Learning this mapping has been heavily investigated in the literature Zhou et al. (2022); Conwell et al. (2021b); Lahner (2022), where most of the approaches conduct a form of deep regression. The study of brain encoding has been advanced by the release of naturalistic neuroscience datasets and benchmarks, with text, audio, image or video stimuli. One of the well established benchmarks that studied how deep networks compare to biological neural systems is the Brain-Score benchmark and framework Schrimpf et al. (2018) which relied on grayscale image stimuli. Another recent well established dataset and benchmark, The Algonauts project Cichy et al. (2019; 2021); Gifford et al. (2023), released datasets and challenges that focused on stimuli as natural objects images Cichy et al. (2019), action videos Cichy et al. (2021); Lahner et al. (2024) and natural scenes Gifford et al. (2023). In these benchmarks, fMRI responses were recorded from different subjects and used to study how the human brain encodes these different kinds of stimuli. In this work, we focus specifically on recorded fMRI data for participants watching short video clips from Mini-Algonauts 2021 Cichy et al. (2021). Other benchmarks were released with video stimuli focus Popham et al. (2021); Lahner et al. (2024), including the extension of the aforementioned dataset and the most recent benchmark, BOLD moments Lahner et al. (2024). BOLD moments provided an exhaustive analysis and an improved dataset, as such we also evaluate on it as part of our study. Recent works have also investigated the ability of deep networks to regress on the brain responses for different stimuli Conwell et al. (2021b); Zhou et al. (2022), where one approach Zhou et al. (2022) focused on video stimuli. However, they mainly worked with single-image deep neural network architectures. In this work, we follow this approach closely, but we focus on studying video understanding models to draw insights on how the brain understands actions and models dynamics. While some works in neuroscience studied the time aspect Zhuang et al. (2021); Nishimoto et al. (2011); Khosla et al. (2021); Nishimoto (2021); Lahner et al. (2024); Güçlü & Van Gerven (2017); Shi et al. (2018); Sinz et al. (2018); Huang et al. (2023), they did not focus on large-scale comparison. Our work focuses on the first study of state-of-the-art deep video understanding models from a neuroscience perspective with more than two million regression fits.

Voxel connectivity encoding models. The brain is an interconnected system with local correlations within one region and global correlations across regions Genç et al. (2016); Li et al. (2022). Few recent works explored the potential of using cortical connectivity in neural encoding models Mell et al. (2021); Xiao et al. (2022). In Mell et al. (2021), they proposed a model that used predefined source voxels as input to predict a target voxel and compared it to the vanilla stimulus-to-voxels prediction models as the standard neural encoding scheme. Nonetheless, these voxels-to-voxels models are not designed to take stimulus as input and define source voxels in an ad hoc manner. Our work is inspired by that direction, yet we propose a fully integrated model that learns a two-stage architecture, stimulus-to-voxels and voxels-to-voxels. More importantly, our approach takes into consideration all voxels from all visual cortex regions and learns the weighting mechanism, instead of relying on ad hoc non learnable mechanism to define source voxels. Another work Xiao et al. (2022) proposed an encoding approach to improve the neural predictions of high-level visual areas using the predictions of low-level visual areas. On the other hand, our method enables learning from all voxels in the same region and other regions at once within a learnable scheme to leverage inter and intra-region connectivity priors. Additionally, our scheme allows for learning from multiple regions and from the same region in one shot, while previous works mainly used connectivity to one paired region. Finally, we are the first to demonstrate the impact of encoding dynamics on utilizing these connectivity priors to improve neural encoding performance.

3 METHOD

In this section, we describe our environment design for the real and the simulated experiments. Then, we discuss the candidate video understanding models and our proposed neural encoding scheme.

3.1 ENVIRONMENT DESIGN

In biological neural systems encoding, we aim to study how different stimuli map to the recorded brain responses. It is usually studied within the framework of aligning and comparing deep network

architectures and biological neural systems. In this case, the biological neural system is considered the target model, and the candidate deep network architecture, that extracts features from the stimuli to be mapped to the brain responses through deep regression, is considered the source model. However, our first goal is to answer the question: "Can we perform system identification for the underlying dynamics encoding scheme?". We use the dynamics encoding to refer to the model's ability to learn from dynamic information provided in an input clip and encode it within the learned representations. To answer that, inspired by previous work Han et al. (2023), we use the features extracted from known architectures as the target, on which we apply our regression, instead of the brain responses as an upper bound. This allows us to identify the dynamics encoding scheme, which serves as a form of ground truth for comparing different models. However, unlike previous work that focused only on studying the architecture (i.e., convolutional *vs.* transformer-based), we go beyond that to study whether models process standalone images or learn dynamics from the input video (i.e. image *vs.* video understanding models).

The second question we aim to study: "How do deep video understanding models families compare to biological neural systems?". Towards this, we study the identification across families of models when encoding the brain responses. Specifically, families are defined based on: (i) the input, whether models learned from single images or videos encouraging them to learn dynamics and motion, (ii) the supervision, whether they are trained in a fully-supervised framework for a certain downstream task or in a self-supervised manner using unlabeled data, and (iii) the architecture, whether the model architecture relies on local convolutional operations or transformer-based global operations. While previous works focused on the architecture aspect, we argue it is even more important to look into whether the model is learning dynamics (e.g., motion) or simply using static information from a single image. Moreover, it is important to understand the impact of the supervision signal used to train the model. Throughout all the experiments we utilize Mini-Algonauts 2021 dataset Cichy et al. (2021), in addition to providing additional results on the BOLD moments dataset Lahner et al. (2024). In the following, we describe the design details of both the simulated environment, where the target is yet another deep network representation, and the real environment, where the target is the visual cortex responses.

Simulated environment. We select four target models from both the image/video understanding models and convolutional-/transformer-based models. Specifically, we use ResNet-50 He et al. (2016), I3D ResNet-50 Carreira & Zisserman (2017), ViT-B Dosovitskiy et al. (2021) and MViT-B Fan et al. (2021b). ResNet-50 and I3D ResNet-50 are convolutional-based models, while ViT-B and MViT-B are transformer-based models. On the other hand, I3D ResNet-50 and MViT-B are video understanding models, while ResNet-50 and ViT-B are single image understanding models. For each target, we use the other candidate models as source. The layers representations are extracted from each target model as detailed in Appendix A, with input videos from Mini-Algonauts. A dimensionality reduction is conducted on these representations for computational efficiency reasons.

Real environment. In the real set of experiments, our target is the brain responses. In this case, we use the public fMRI datasets from Mini-Algonauts and BOLD moments Cichy et al. (2021); Lahner et al. (2024). We mainly use the training set, and perform cross-validation over four folds throughout all our experiments. The dataset provides fMRI recordings of ten subjects who watched short video clips of three seconds average duration. Each video and voxel in the brain was represented by a single activation value. In Mini-Algonauts 2021 dataset, we use the brain responses from nine regions of interest of the visual cortex, these are across two levels: (i) early and mid-level visual cortex (V1, V2, V3, and V4), and (ii) high-level visual cortex (EBA, FFA, STS, LOC, and PPA). The early and mid-level visual cortex regions are concerned with lower-level features such as orientations and frequencies, while the high-level ones are concerned with semantics in terms of objects, scenes, bodies, and faces. We also conduct the same study on BOLD moments with a comprehensive 46 cortical regions that is described in the appendix B.1. The datasets we use is provided at TR one second and has shown sensitivity to the temporal ordering of information in the video stimuli Lahner et al. (2024). This motivates our choice for the two datasets when studying video understanding models and their relation to the visual cortex when encoding dynamics.

3.2 CANDIDATE MODELS

Here we describe the candidate models that are used in our experiments. We choose to run our experiments on more than 35 source models, listed in Table 1, with their model family and configurations.

Table 1: List of the candidate models and their families and configurations that were used during their training. We list the backbone/s, the training datasets, and the configuration as clip length × sampling rate. For the training datasets we use ImageNet Deng et al. (2009) (IN), Kinetics-400 Kay et al. (2017) (K400), Charades Sigurdsson et al. (2016) (Ch) and Something-something v2 Goyal et al. (2017) (SSV2).

Input	Supervision	Architecture	Network (Backbone/s - Dataset/s - Config.)
Video	Fully-supervised	Convolutional	C2D (R50-K400-8 × 8)
			CSN (R101-K400-32 × 2)
			I3D (R50-K400-8 × 8)
			R(2+1)D (R50-K400-16 × 4)
			SlowFast (R50,101-K400,Ch,SSV2-8 × 8,4 × 16)
			3DResNet (R18,50-K400,Ch,SSV2-8 × 8,4 × 16)
			X3D (XS,S,M,L-K400-Matched Sampling Rate)
		Transformers	MViT (B-K400-16 × 4,32 × 3)
			TimeSformer (B-K400,SSV2-8 × 8)
			OmniMAE finetuned (B-SSV2-8 × 8)
	Self-supervised	Transformers	stMAE (L-K400-8 × 8)
			OmniMAE (B,L-IN/SSV2-8 × 8)
Image	Fully-supervised	Convolutional	ResNet (R152,101,50,34,18-IN-8 × 8)
		Transformers	ViT (B16,32,L16,32-IN-8 × 8)
	Self-supervised	Transformers	DINO (B-IN-8 × 8)
			MAE (B-IN-8 × 8)

Video understanding models include C2D Li et al. (2019), CSN Tran et al. (2019), I3D Carreira & Zisserman (2017), R(2+1)D Tran et al. (2018), SlowFast, the Slow branch (3D ResNet-50) Feichtenhofer et al. (2019), X3D Feichtenhofer (2020), MViT Fan et al. (2021b) and TimeSformer Bertasius et al. (2021). Self-supervised video understanding models, stMAE Feichtenhofer et al. (2022) and OmniMAE Girdhar et al. (2023) are used as well. We mainly focus on the models that showed state of the art performance in action recognition. Single image understanding models include ResNets He et al. (2016), ViTs Dosovitskiy et al. (2021) and the self-supervised DINO Caron et al. (2021) and MAE He et al. (2022). Families of models are categorized based on the input, supervision and architecture type as discussed earlier. We detail the number of layers and which layers are sampled for each deep network used in Appendix A.

3.3 ENCODING TECHNIQUE

Inspired by the recent work Zhou et al. (2022), we use a layer-weighted region of interest encoding that takes the hierarchical nature of deep networks into consideration. Initially, we sample the frames from a video to obtain the input clip. For image understanding models we extract features per frame, while for video ones we extract features from the entire clip at once. Then, we pre-process the input features from the different layers of a candidate model through averaging the features on the temporal dimension. This is followed by performing sparse random projection Li et al. (2006) for dimensionality reduction and computational efficiency reasons. Assume input features for layer, l, after dimensionality reduction as, $X_l \in \mathbb{R}^{C \times 1}$, with C features. We learn the weights of one fully connected layer to provide the predictions of the voxels of one region of interest in the visual cortex as, $\hat{Y}_l = W_l X_l$. Where $W_l \in \mathbb{R}^{N \times C}$, $\hat{Y} \in \mathbb{R}^{N \times 1}$ and N is the number of voxels in the region of interest. Instead of a simple ridge regression, we learn a weighted sum of the predictions of all layers and use the following loss to train our regression model,

$$\mathcal{L} = \|Y - \sum_{l=1}^{L} \omega_l \hat{Y}_l\|_2^2 + \beta_1 \sum_{l=1}^{L} \|W_l\|_2 + \beta_2 \|\omega\|_1, \tag{1}$$

where ω_l is a learnable scalar weight for layer, l, and, ω, is the vector of weights. Each ω_l, controls the contribution of layer, l, to the final regression of the region of interest, and β_1, β_2 are hyper-parameters of the regularization. We use L1 regularization for the layer weights to enforce sparsity. This encoding scheme avoids unnecessary assumptions that there is a one-to-one alignment between layers and visual brain regions of interest. Accordingly, this encoding scheme allows for more complex interactions among the layers and the brain regions of interest.
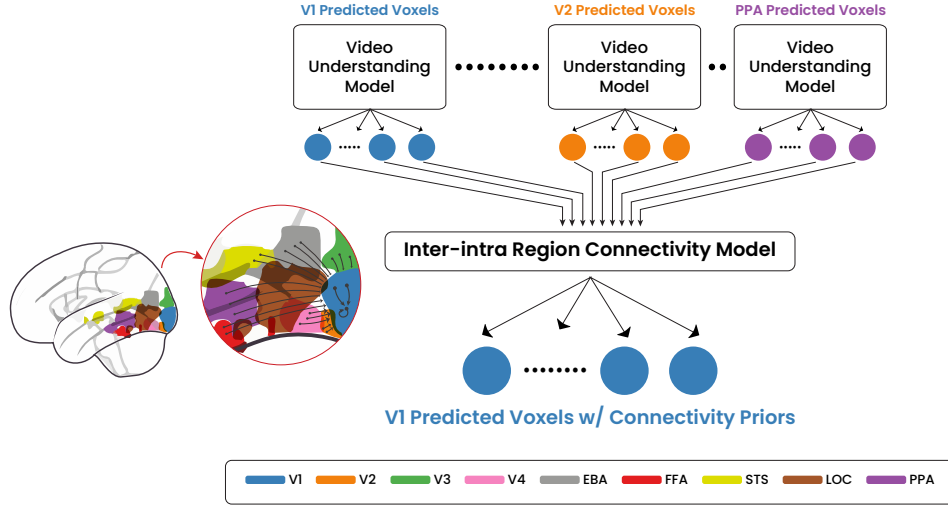
Figure 1: Architecture of our dynamics based neural encoding with inter-intra region connectivity priors. Our fully integrated model learns the connectivity from all regions voxels (inter-region) and all voxels in the same region (intra-region). We only show one target region, V1, as an illustration where we use the same mechanism across all regions. Note the arrows thickness, in our visual cortex regions illustration, indicate the degree of connectivity corresponding to the computed in Fig. 5c.

3.4 INTER-INTRA REGION CONNECTIVITY PRIORS

In this section, we present a novel encoding scheme on top of the best-performing video understanding models by fully integrating the neural encoding with inter- and intra-region voxel connectivity priors. An overview of our architecture is shown in Fig. 1. The input video stimuli goes through the source video understanding model to extract multiple layers features as described in Sec. 3.3, followed by the connectivity module which takes the concatenated voxels of the nine visual regions as input. This module consists of four layers: two fully-connected coupled with L2 regularization and two dropout ones. Finally, the output of the model is the predicted voxels of a single visual region. We train our model in a two-stage fashion, where we train the standard neural encoding scheme without connectivity, followed by training the connectivity module. In the training phase, the main target is to learn the connectivity between the voxels of all the regions and the target region including intra-connectivity between the voxels of the target region itself and the inter-connectivity between voxels of the target region and the other visual regions. Accordingly, in the training phase, the input to the model is the groundtruth voxel activations. However, in the inference phase, the input to the model is the predicted voxel activations.

4 EXPERIMENTAL RESULTS

4.1 IMPLEMENTATION DETAILS

In this subsection, we describe our experiment design and implementation details. The input clips to all models are constructed based on a sampling rate that corresponds to the sampling rate used during its training for video understanding models. As for image understanding models we use the default sampling rate of eight. The clip length is computed based on the sampling rate and the input video length and changes according to the video length.

Before training the regressor, a hyperparameter tuning is conducted using two-fold cross-validation on the training set of the first subject, following previous work Zhou et al. (2022). The two main hyper-parameters we tune are the β_1, β_2, using grid search $\beta_1 \in \{0.1, 1, 10\}$ and $\beta_2 \in \{1, 10, 100\}$. Moreover, an early-stopping strategy is employed through the hyperparameter tuning and training phases. The main metric used throughout the experiments is the average Pearson's correlation
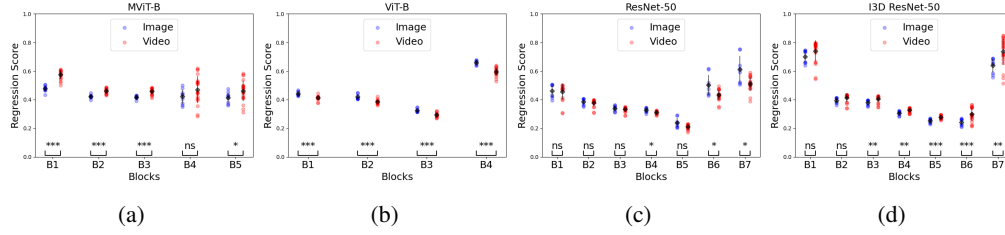
Figure 2: Simulated experiments showing regression scores as Pearson's correlation coefficient of image (blue) *vs.* video (red) model families on four target models; (a) MViT-B, (b) ViT-B, (c) ResNet-50, (d) I3D ResNet-50. We show the regression on the target network output features from their respective blocks, B0-7. Statistical significance is shown at the bottom as 'ns' not significant, '$*, **, ***$' significant with p-values $< 0.05, 0.01, 0.001$, resp. It shows higher regression scores for the model family corresponding to the target network, especially in MViT and ViT.

coefficient across all voxels within a specific region in the brain. All results are averaged over the subjects. We conduct experiments on four folds and report the average and standard deviation. We report the statistical significance across families of models using Welch's t-test. The real setup, in which the human visual cortex is the target, is conducted on the Mini-Algonouts 2021 dataset Cichy et al. (2019), additional results on BOLD moments dataset is provided in Appendix B.1. In each fold of the four folds we used in our experiments, the 1,000 videos are split into training and testing sets as 90% and 10%, respectively. In the simulated setup, we follow the same setup for the real environment. All the previous models are trained on A6000 GPU with training span of one day average per regression model.

4.2 CAN WE PERFORM SYSTEM IDENTIFICATION WITH RESPECT TO THE DYNAMICS ENCODING?

We first investigate the question of whether system identification of single image *vs.* video understanding models is possible. Figure 2 shows that for MViT and ViT target models, the correct family of models is better able to represent each. Specifically, we observe higher regression scores of the video understanding models for MViT and the single image one for ViT. Note that we include video understanding models that are trained on three different datasets which are Kinetics, Charades, and Something-Something v2 to ensure the results are not dependent on a certain training dataset.

When inspecting ResNet-50 as a target, we observe the mean of image understanding models is higher, but is only statistically significant in three layers. When looking at I3D target model, we notice the mean of video understanding models is higher and is statistically significant except in early layers. In summary, we have demonstrated that system identification can be attained to a certain level with most of the layers showing statistical significance. Additional simulated experiments are provided in Appendix B.2. In the following section we investigate the same but for the unknown biological neural system.

4.3 HOW DO DEEP VIDEO UNDERSTANDING MODELS FAMILIES COMPARE TO THE HUMAN VISUAL CORTEX?

In this section, we focus on the real experiments, where the target model is the biological neural system, to understand the underlying mechanisms of the visual cortex. We conduct three comparisons; single image *vs.* video understanding families of models, convolutional-based *vs.* transformer-based models, and fully-supervised *vs.* self-supervised models. Figure 3a clearly demonstrates that across most brain regions, video understanding models have better capability to model the visual cortex responses than single image architectures. We believe the reason behind this is that the brain is encoding the dynamics occurring in a video similar to the encoded dynamics in video understanding models more than what occurs in single image understanding models. Figure 3b shows the comparison between transformer-based and convolutional-based models. It shows that convolutional models have higher regression scores across early-mid regions in the visual cortex with relatively high statistical significance. This difference decrease as we go to higher level regions until it becomes insignificant. Interestingly, it has been noted in recent works that transformers lack the ability to
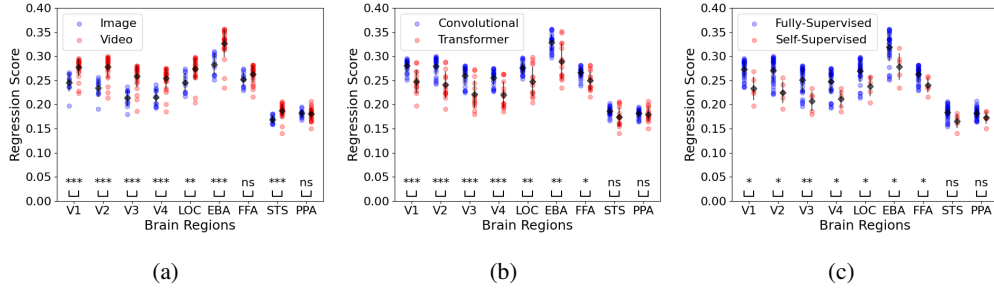
Figure 3: Real experiments showing regression scores as Pearson's correlation coefficient of model families on brain fMRI data. Comparison between: (a) image *vs.* video understanding models, (b) convolutional *vs.* transformer-based models and (c) fully supervised *vs.* self-supervised models. Statistical significance is shown in the bottom as 'ns' not significant, '$*, **, ***$' significant with p-values $< 0.05, 0.01, 0.001$, resp. It shows video understanding models outperform single image ones, fully supervised outperform self supervised ones and convolutional models surpass transformer based ones in early-mid regions.

capture high-frequency components Bai et al. (2022). On the other hand, early layers in convolutional models tend to capture high-frequency components by detecting oriented gradients. This also might relate to empirical results that demonstrated vision transformers with shallow convolutional stem (i.e., three convolutional layers) perform better than the ones that directly take patches as input Xiao et al. (2021). As such, brain modelling in the early and mid regions of the visual cortex relates better to convolutional-based models, since they better capture high-frequency components. Nonetheless, we notice the best model in the transformer based family, MViT, tends to behave similar to convolutional ones in early-mid regions unlike other transformer based architectures. Additional results in Appendix B.2 are provided to confirm the previous insight. Surprisingly, Fig. 3c shows that fully-supervised models are better able to predict most of the regions than self-supervised models. Appendix B.1 provides the results of the previous study conducted on BOLD moments dataset across 46 regions, which confirms the consistency of our main findings across different datasets. Moreover, Appendix B.3 shows the model subfamilies while focusing only on the video understanding models and excluding the single image models, in addition to comparing convolutional *vs.* transformer based models that are trained with full supervision only.

4.4 Fine-grained analysis

In this section, we conduct a fine-grained analysis that goes beyond families of models. We start with studying two stream *vs.* single stream architectures across three video understanding datasets. Figure 4a shows that the two stream architectures have better ability to model the visual cortex than single stream ones in the low level regions and are either better or on-par in the high level regions. We then discuss the self-supervised learning results that showed worse regression scores in comparison to full supervision. Towards this end, we investigate OmniMAE variants (i.e., self supervised and finetuned) and TimeSformer. Figure 4b shows that fully supervised models give better scores than the self-supervised ones across the nine regions. We leave the reasons behind this result as an open question for future research on why fully supervised models tend to align better with the cortical responses than self supervised ones. Furthermore, we investigate which models are better at predicting the visual cortex responses. Figure 4c shows that both SlowFast, a two-stream architecture, and MViT, a multiscale vision transformer, are the best in modelling the visual cortex across the nine regions. SlowFast which is a convolutional approach is comparable to MViT with difference that is statistically not significant across all regions. Moreover, we see self-supervised models (i.e., stMAE and OmniMAE) lagging behind fully supervised ones. Additional analysis is provided in Appendix B.4 and B.5.

4.5 Inter-intra region connectivity

In this section, we show the results of our improved neural encoding mechanism that builds upon the best video understanding models (MViT-B and SlowFast) while incorporating intra- and inter-region
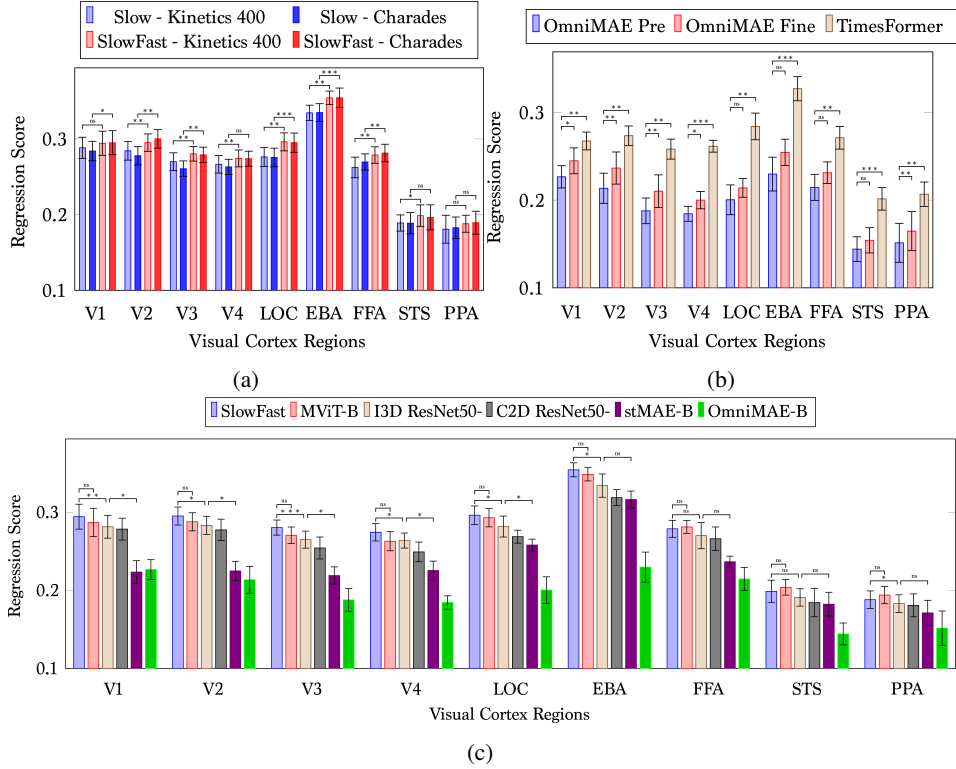
Figure 4: Fine-grained analysis of the video understanding models across the nine regions of the human visual cortex showing the Pearson's correlation coefficient as the regression scores. (a) Single stream *vs.* two stream SlowFast architectures. (b) OmniMAE pre-trained in a self-supervised manner *vs.* TimeSformer and OmniMAE fine-tuned with full supervision. All models are based on ViT-B and trained on SSV2. (c) Comparison between six video understanding models. Statistical significance is shown on top of bar pairs as 'ns' not significant, '$*, **, ***$' significant with p-values $< 0.05, 0.01, 0.001$, resp.

connectivity. Figure 5a shows the statistically significant enhancements in prediction accuracy in both MViT-B and SlowFast models after incorporating voxel-connectivity to their predictions. These results show that integrating the intra- and inter-connectivity across the visual regions is an important component for a better neural encoding. As an ablation study, we examine the performance enhancement in MViT-B in the case of intra-connectivity or inter-connectivity separately. Figure 5b shows that the full-connectivity (i.e., combining both) is either superior or on-par with intra-connectivity or inter-connectivity standalone. To better understand the directional connectivity between the regions, we analyze the average learned weights of each region as contributors to the MViT-B accuracy enhancement of each target visual region as shown in Figure 5c. It shows the following: i) the effect of one region on another is not symmetric but directional, ii) early-mid regions (V1, V2, V3, and V4) are the highest contributors to the accuracy enhancement of other early-mid regions, and the same for late-regions (LOC, EBA, FFA, STS, and PPA), iii) V4 is contributing to both early-mid and late regions, and iv) the contributions of late regions on early regions (V1, V2) are stronger than contribution of early regions on late regions which could be attributed to the top-down influence of feedback-pathways in the visual cortex Gilbert & Li (2013).

Finally, we perform an ablation of the improvement from intra- and inter-region connectivity prior when using an image understanding model *vs.* a video understanding one. Figure 6a illustrates the effect of inter-intra region connectivity priors on a single image understanding model (ResNet-50), where we show that it improves over the baseline with no connectivity across most of the regions with statistical significance. More importantly, we study the gain from the connectivity priors with that single image understanding model (ResNet-50) *vs.* a video understanding model that learns dynamics (MViT). Figure 6b shows that the gain from MViT is on average higher than the ResNet-50 across all the regions. When looking upon the statistical significance of these results, we notice almost half of the regions show a significant gain from encoding dynamics over the single image understanding
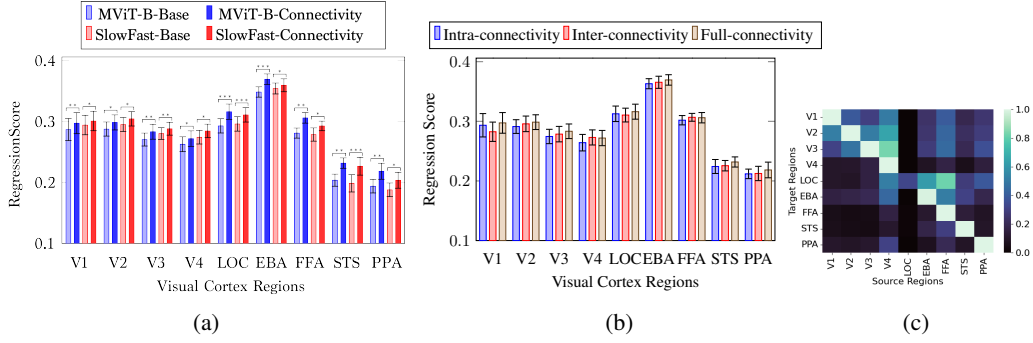
Figure 5: (a) Comparison of base model accuracies of MViT-B-16x4 and SlowFast and their accuracies after incorporating the intra-region and inter-region voxel connectivity showing the Pearson's correlation coefficient as the regression scores. It shows the superiority of the connectivity based models. (b) Comparison of performance enhancement by incorporating the intra-region and inter-region voxel connectivity together or each of them separately showing the Pearson's correlation coefficient as the regression scores. It confirms on the need for combining both intra- and inter-region connectivity. (c) Average weights per region contributing to the accuracy enhancement of each target visual region, showing the directional learned connectivity in our model.
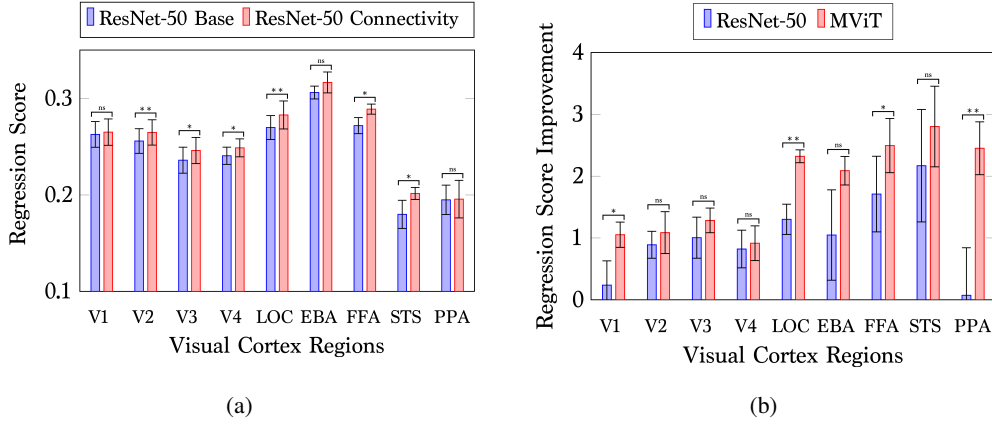

Figure 6: (a) Comparison of base model accuracy of ResNet-50 and its accuracy after incorporating the inter-intra region voxel connectivity showing the Pearson's correlation coefficient as the regression scores. (b) Comparison of improvement in the regression scores in ResNet-50 *vs.* MViT w/ connectivity priors. Difference in regression scores (i.e., Pearson correlation coefficient) is shown in a different scale after multiplying by 100 for visualization. It confirms that the dynamics based encoding improves the benefit from connectivity priors.

baseline. Hence, we show in these results that the dynamics encoding in video understanding models reinforces the connectivity priors. We refer to additional ablations that compares our learned connectivity to a random or an identity one in Appendix B.6, again confirming on the benefit of our learned connectivity.

4.6 SUMMARY

In summary: (i) Simulated results show that system identification between image and video understanding models is attainable to a certain level. (ii) We show that video understanding models are better in regressing the visual cortex responses than image ones. (iii) We show that convolutional models predict better the early-mid regions than transformer based ones. (iv) We show that MViT, with its multiscale processing, tends to perform similar to convolutional models in early-mid regions. (v) We show that two-stream models perform better than single stream. (vi) We show that models trained with full supervision surpass the ones with self supervision. (vii) Finally, we demonstrate a

better neural encoding scheme that utilizes both encoded dynamics and inter-intra region connectivity. We refer to Appendix C and D for a discussion on the limitations and broader impact.

5 Conclusion

This paper has provided a large-scale study of video understanding models from a neuroscience perspective. We have shown the feasibility of system identification for single image *vs.* video understanding models. Moreover, we have shown that modelling dynamics should be considered when comparing biological neural system responses to deep networks and provided insights on different families of models. Finally, we showcased the interplay of dynamics modelling and inter-intra region connectivity in neural encoding.

6 Acknowledgements

References

Jiawang Bai, Li Yuan, Shu-Tao Xia, Shuicheng Yan, Zhifeng Li, and Wei Liu. Improving vision transformers by revisiting high-frequency components. In *Proceedings of the European Conference on Computer Vision*, pp. 1–18. Springer, 2022.

Gedas Bertasius, Heng Wang, and Lorenzo Torresani. Is space-time attention all you need for video understanding? In *Proceedings of the International Conference on Machine Learning*, volume 2, pp. 4, 2021.

Mathilde Caron, Hugo Touvron, Ishan Misra, Hervé Jégou, Julien Mairal, Piotr Bojanowski, and Armand Joulin. Emerging properties in self-supervised vision transformers. In *Proceedings of the IEEE/CVF International Conference on Computer Vision*, pp. 9650–9660, 2021.

Joao Carreira and Andrew Zisserman. Quo vadis, action recognition? a new model and the kinetics dataset. In *Proceedings of the IEEE Conference on Computer Vision and Pattern Recognition*, pp. 6299–6308, 2017.

Radoslaw Martin Cichy, Gemma Roig, and Aude Oliva. The algonauts project. *Nature Machine Intelligence*, 1(12):613–613, 2019.

Radoslaw Martin Cichy, Kshitij Dwivedi, Benjamin Lahner, Alex Lascelles, Polina Iamshchinina, M Graumann, Alex Andonian, NAR Murty, K Kay, Gemma Roig, et al. The algonauts project 2021 challenge: How the human brain makes sense of a world in motion. *arXiv preprint arXiv:2104.13714*, 2021.

Colin Conwell, David Mayo, Andrei Barbu, Michael Buice, George Alvarez, and Boris Katz. Neural regression, representational similarity, model zoology & neural taskonomy at scale in rodent visual cortex. *Advances in Neural Information Processing Systems*, 34:5590–5607, 2021a.

Colin Conwell, Jacob S Prince, George A Alvarez, and Talia Konkle. What can 5.17 billion regression fits tell us about artificial models of the human visual system? In *Shared Visual Representations in Human and Machine Intelligence workshop at Conference on Neural Information Processing Systems*, 2021b.

Jia Deng, Wei Dong, Richard Socher, Li-Jia Li, Kai Li, and Li Fei-Fei. ImageNet: A large-scale hierarchical image database. In *2009 IEEE Conference on Computer Vision and Pattern Recognition*, pp. 248–255. Ieee, 2009.

Alexey Dosovitskiy, Lucas Beyer, Alexander Kolesnikov, Dirk Weissenborn, Xiaohua Zhai, Thomas Unterthiner, Mostafa Dehghani, Matthias Minderer, Georg Heigold, Sylvain Gelly, Jakob Uszkoreit, and Neil Houlsby. An image is worth 16x16 words: Transformers for image recognition at scale. In *International Conference on Learning Representations*, 2021.

Haoqi Fan, Tullie Murrell, Heng Wang, Kalyan Vasudev Alwala, Yanghao Li, Yilei Li, Bo Xiong, Nikhila Ravi, Meng Li, Haichuan Yang, et al. Pytorchvideo: A deep learning library for video understanding. In *Proceedings of the 29th ACM international conference on multimedia*, pp. 3783–3786, 2021a.

Haoqi Fan, Bo Xiong, Karttikeya Mangalam, Yanghao Li, Zhicheng Yan, Jitendra Malik, and Christoph Feichtenhofer. Multiscale vision transformers. In *Proceedings of the IEEE/CVF International Conference on Computer Vision*, pp. 6824–6835, 2021b.

Christoph Feichtenhofer. X3d: Expanding architectures for efficient video recognition. In *Proceedings of the IEEE/CVF Conference on Computer Vision and Pattern Recognition*, pp. 203–213, 2020.

Christoph Feichtenhofer, Haoqi Fan, Jitendra Malik, and Kaiming He. Slowfast networks for video recognition. In *Proceedings of the IEEE/CVF International Conference on Computer Vision*, pp. 6202–6211, 2019.

Christoph Feichtenhofer, Yanghao Li, Kaiming He, et al. Masked autoencoders as spatiotemporal learners. *Advances in Neural Information Processing Systems*, 35:35946–35958, 2022.

Erhan Genç, Marieke Louise Schölvinck, Johanna Bergmann, Wolf Singer, and Axel Kohler. Functional connectivity patterns of visual cortex reflect its anatomical organization. *Cerebral cortex*, 26 (9):3719–3731, 2016.

Alessandro T Gifford, Benjamin Lahner, Sari Saba-Sadiya, Martina G Vilas, Alex Lascelles, Aude Oliva, Kendrick Kay, Gemma Roig, and Radoslaw M Cichy. The algonauts project 2023 challenge: How the human brain makes sense of natural scenes. *arXiv preprint arXiv:2301.03198*, 2023.

Charles D Gilbert and Wu Li. Top-down influences on visual processing. *Nature Reviews Neuroscience*, 14(5):350–363, 2013.

Rohit Girdhar, Alaaeldin El-Nouby, Mannat Singh, Kalyan Vasudev Alwala, Armand Joulin, and Ishan Misra. Omnimae: Single model masked pretraining on images and videos. In *Proceedings of the IEEE/CVF Conference on Computer Vision and Pattern Recognition*, pp. 10406–10417, 2023.

Raghav Goyal, Samira Ebrahimi Kahou, Vincent Michalski, Joanna Materzynska, Susanne Westphal, Heuna Kim, Valentin Haenel, Ingo Fruend, Peter Yianilos, Moritz Mueller-Freitag, et al. The" something something" video database for learning and evaluating visual common sense. In *Proceedings of the IEEE international conference on computer vision*, pp. 5842–5850, 2017.

Umut Güçlü and Marcel AJ Van Gerven. Modeling the dynamics of human brain activity with recurrent neural networks. *Frontiers in computational neuroscience*, 11:7, 2017.

Yena Han, Tomaso A Poggio, and Brian Cheung. System identification of neural systems: If we got it right, would we know? In *International Conference on Machine Learning*, pp. 12430–12444. PMLR, 2023.

Kaiming He, Xiangyu Zhang, Shaoqing Ren, and Jian Sun. Deep residual learning for image recognition. In *Proceedings of the IEEE Conference on Computer Vision and Pattern Recognition*, pp. 770–778, 2016.

Kaiming He, Xinlei Chen, Saining Xie, Yanghao Li, Piotr Dollár, and Ross Girshick. Masked autoencoders are scalable vision learners. In *Proceedings of the IEEE/CVF Conference on Computer Vision and Pattern Recognition*, pp. 16000–16009, 2022.

Liwei Huang, ZhengYu Ma, Huihui Zhou, and Yonghong Tian. Deep recurrent spiking neural networks capture both static and dynamic representations of the visual cortex under movie stimuli. *arXiv preprint arXiv:2306.01354*, 2023.

Will Kay, Joao Carreira, Karen Simonyan, Brian Zhang, Chloe Hillier, Sudheendra Vijayanarasimhan, Fabio Viola, Tim Green, Trevor Back, Paul Natsev, et al. The kinetics human action video dataset. *arXiv preprint arXiv:1705.06950*, 2017.

Meenakshi Khosla, Gia H Ngo, Keith Jamison, Amy Kuceyeski, and Mert R Sabuncu. Cortical response to naturalistic stimuli is largely predictable with deep neural networks. *Science Advances*, 7(22):eabe7547, 2021.

Benjamin Lahner. *An fMRI dataset of 1,102 natural videos for visual event understanding*. PhD thesis, Massachusetts Institute of Technology, 2022.

Benjamin Lahner, Kshitij Dwivedi, Polina Iamshchinina, Monika Graumann, Alex Lascelles, Gemma Roig, Alessandro Thomas Gifford, Bowen Pan, SouYoung Jin, N Apurva Ratan Murty, et al. Modeling short visual events through the bold moments video fmri dataset and metadata. *Nature communications*, 15(1):6241, 2024.

Chao Li, Qiaoyong Zhong, Di Xie, and Shiliang Pu. Collaborative spatiotemporal feature learning for video action recognition. In *Proceedings of the IEEE/CVF Conference on Computer Vision and Pattern Recognition*, pp. 7872–7881, 2019.

Ping Li, Trevor J Hastie, and Kenneth W Church. Very sparse random projections. In *Proceedings of the International Conference on Knowledge Discovery and Data Mining*, pp. 287–296, 2006.

Yuanning Li, Huzheng Yang, and Shi Gu. Upgrading voxel-wise encoding model via integrated integration over features and brain networks. *BioRxiv*, pp. 2022–11, 2022.

Maggie Mae Mell, Ghislain St-Yves, and Thomas Naselaris. Voxel-to-voxel predictive models reveal unexpected structure in unexplained variance. *NeuroImage*, 238:118266, 2021.

Shinji Nishimoto. Modeling movie-evoked human brain activity using motion-energy and space-time vision transformer features. *BioRxiv*, pp. 2021–08, 2021.

Shinji Nishimoto, An T Vu, Thomas Naselaris, Yuval Benjamini, Bin Yu, and Jack L Gallant. Reconstructing visual experiences from brain activity evoked by natural movies. *Current biology*, 21(19):1641–1646, 2011.

Adam Paszke, Sam Gross, Francisco Massa, Adam Lerer, James Bradbury, Gregory Chanan, Trevor Killeen, Zeming Lin, Natalia Gimelshein, Luca Antiga, et al. Pytorch: An imperative style, high-performance deep learning library. *Advances in neural information processing systems*, 32, 2019.

Sara F Popham, Alexander G Huth, Natalia Y Bilenko, Fatma Deniz, James S Gao, Anwar O Nunez-Elizalde, and Jack L Gallant. Visual and linguistic semantic representations are aligned at the border of human visual cortex. *Nature neuroscience*, 24(11):1628–1636, 2021.

Martin Schrimpf, Jonas Kubilius, Ha Hong, Najib J Majaj, Rishi Rajalingham, Elias B Issa, Kohitij Kar, Pouya Bashivan, Jonathan Prescott-Roy, Franziska Geiger, et al. Brain-score: Which artificial neural network for object recognition is most brain-like? *BioRxiv*, pp. 407007, 2018.

Junxing Shi, Haiguang Wen, Yizhen Zhang, Kuan Han, and Zhongming Liu. Deep recurrent neural network reveals a hierarchy of process memory during dynamic natural vision. *Human brain mapping*, 39(5):2269–2282, 2018.

Gunnar A Sigurdsson, Gül Varol, Xiaolong Wang, Ali Farhadi, Ivan Laptev, and Abhinav Gupta. Hollywood in homes: Crowdsourcing data collection for activity understanding. In *Proceedings of the European Conference on Computer Vision*, pp. 510–526. Springer, 2016.

Fabian Sinz, Alexander S Ecker, Paul Fahey, Edgar Walker, Erick Cobos, Emmanouil Froudarakis, Dimitri Yatsenko, Zachary Pitkow, Jacob Reimer, and Andreas Tolias. Stimulus domain transfer in recurrent models for large scale cortical population prediction on video. *Advances in neural information processing systems*, 31, 2018.

Du Tran, Heng Wang, Lorenzo Torresani, Jamie Ray, Yann LeCun, and Manohar Paluri. A closer look at spatiotemporal convolutions for action recognition. In *Proceedings of the IEEE Conference on Computer Vision and Pattern Recognition*, pp. 6450–6459, 2018.

Du Tran, Heng Wang, Lorenzo Torresani, and Matt Feiszli. Video classification with channel-separated convolutional networks. In *Proceedings of the IEEE/CVF International Conference on Computer Vision*, pp. 5552–5561, 2019.

Tete Xiao, Mannat Singh, Eric Mintun, Trevor Darrell, Piotr Dollár, and Ross Girshick. Early convolutions help transformers see better. *Advances in Neural Information Processing Systems*, 34: 30392–30400, 2021.

Wulue Xiao, Jingwei Li, Chi Zhang, Linyuan Wang, Panpan Chen, Ziya Yu, Li Tong, and Bin Yan. High-level visual encoding model framework with hierarchical ventral stream-optimized neural networks. *Brain Sciences*, 12(8):1101, 2022.

Qiongyi Zhou, Changde Du, and Huiguang He. Exploring the brain-like properties of deep neural networks: a neural encoding perspective. *Machine Intelligence Research*, 19(5):439–455, 2022.

Chengxu Zhuang, Siming Yan, Aran Nayebi, Martin Schrimpf, Michael C Frank, James J DiCarlo, and Daniel LK Yamins. Unsupervised neural network models of the ventral visual stream. *Proceedings of the National Academy of Sciences*, 118(3):e2014196118, 2021.

Table 2: Detailed description per architecture of the used layers.

Architecture	# Layers	Sampled Layers
CSN, R(2+1)D, 3DResNet	6	5 convolutional blocks and last fully connected layer
C2D, I3D	7	5 convolutional blocks, max pooling and last fully connected layer
SlowFast	12	5 convolutional blocks for each branch (slow & fast) and the last 2 layers combined
X3D	6	5 convolutional blocks and last fully connected layer
ViT, TimeSformer	4	Grouped 3 blocks, each block 4 layers and last fully connected layer
Dino - B	4	3 Grouped blocks (4 layers) and CLS token
ResNet	7	5 convolutional blocks, average pooling and last fully connected layer
MViT	5	Grouped 4 blocks (4 layers) and last fully connected layer
OmniMAE, MAE	3	Grouped 3 blocks (4 layers)
stMAE	6	Grouped 6 blocks (4 layers)

A   CANDIDATE MODELS DETAILS

In this section, we provide details on the layers extracted from each of our candidate models in Table 2. Note that for transformer-based architectures instead of using all layers to be selected we rather group layers into blocks of four layers for efficiency reasons and we noticed it gave better results than learning the regression with all input layers at once. Also note that OmniMAE finetuned is trained for the action recognition task on SSV2 dataset Goyal et al. (2017).

B   ADDITIONAL RESULTS

B.1   BOLD MOMENTS DATASET (BMD) RESULTS

In this section, we evaluate on the newly released BOLD Moments Dataset (BMD) Lahner et al. (2024), with fMRI recording of ten subjects watching 1,000 training video stimuli. The dataset provides a preprocessed version (named "Version B") with additional flexibility in the region of interest (ROIs) format. In "Version B" of BMD, 46 regions are defined including right/left hemispheres and ventral/dorsal streams. The defined ROIs include: early visual regions (V1v, V1d, V2v, V2d, V3v, V3d, hV4), a body-selective region (EBA), an object-selective region (LOC), face-selective regions (FFA, OFA, STS), scene-selective regions (PPA, RSC, TOS), additional ROIs (V3ab, IPS0, IPS1-2-3, 7AL, BA2, PFt, and PFop), and finally the motion selective MT ROI. All these ROIs were defined in both right and left hemispheres forming in total 46 ROIs. To further show the robustness of our results and insights, we evaluate all our models using this preprocessed version across the 46 ROIs using cross-validation on 4 folds as shown in Fig. 7. It confirms the consistency of the results previously shown in Fig. 3. Figure 7a confirms the statistically significant superiority of video understanding models compared to single-image models in the majority of cortical regions. Figure 7b confirms that convolutional-based models are better than transformer-based models in representing early-mid visual cortex regions. Finally, Fig. 7c confirms that fully-supervised models perform better than self-supervised ones in predicting activity of most of the visual cortex regions with statistical significance.

B.2   ADDITIONAL SIMULATED EXPERIMENTAL RESULTS

Although our focus in the system identification is on the ability to differentiate image *vs.* video understanding models, we provide additional results for other families of models. In Fig. 8, we show

(a)

(b)

(c)

Figure 7: Real experiments showing regression scores as Pearson's correlation coefficient of model families on brain fMRI data using the BMD dataset. (a) Comparison of image *vs.* video understanding models, (b) comparison of convolutional *vs.* transformer-based models and (c) comparison of fully supervised *vs.* self-supervised models. Statistical significance is shown in the bottom as 'ns' not significant, '$*, **, ***$' significant with p-values $< 0.05, 0.01, 0.001$, resp.
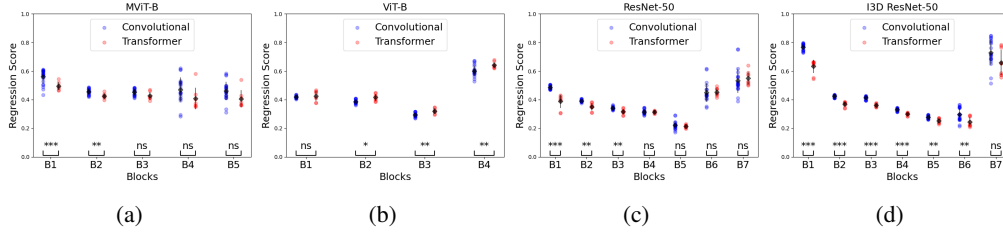
Figure 8: Simulated experiments showing regression scores as Pearson's correlation coefficient of (a-d) convolutional (blue) *vs.* transformer (red) model families on four target models MViT-B 16x4, ViT-B, ResNet-50, and I3D ResNet-50, respectively. Statistical significance is shown at the bottom as 'ns' not significant, '$*, **, * * *$' significant with p-values $< 0.05, 0.01, 0.001$, respectively.
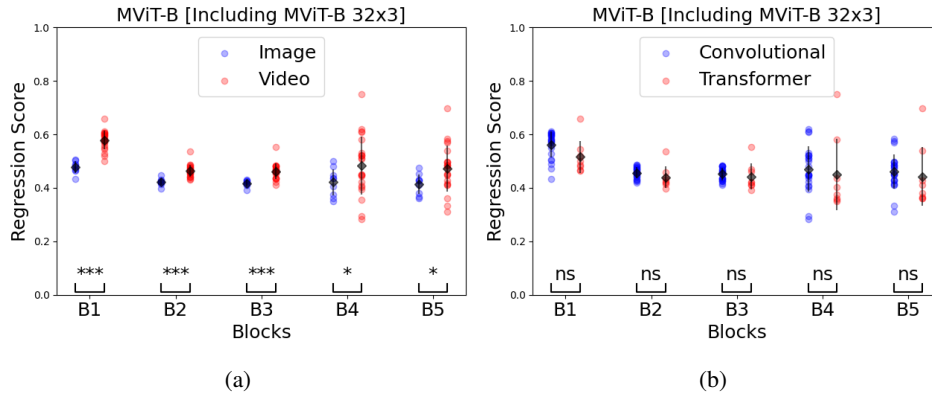

Figure 9: Simulated experiments for MViT-B 16x4 target model after including MViT-B 32x3. Statistical significance is shown at the bottom as 'ns' not significant, '$*, **, * * *$' significant with p-values $< 0.05, 0.01, 0.001$, respectively.

the simulated results comparing convolutional *vs.* transformer based models for four target models MViT-B 16x4, ViT-B, ResNet-50, and I3D ResNet-50, respectively. For the target model I3D, the figure clearly shows that convolutional models are better predictors than transformer-based ones with statistical significance across blocks except the last one. The target model ResNet50 shows that convolutional models are significantly better than transformer-based ones in the early blocks, but the differences are not significant in the late blocks. For ViT-B, the transformer-based models are significantly better than the convolutional models in all the blocks except for the first block which has non-significant difference between the two families. This result is consistent with the results presented in Han et al. (2023). The target model MViT-B shows a surprising result, that is confirming with previous findings in the real experiments as well as detailed in Section B.4, where convolutional models are better in regressing the multiscale variant than transformer-based ones with significant differences in the first two blocks. This might be related to how the multiscale ViT tends to act similar to the convolutional models when predicting early-mid regions of the visual cortex.

In the MViT target model results showed in Fig. 2a and Fig. 8a, we did not include the MViT-32x3 variant for fair comparison between model families given that MViT-32x3 share the same architecture as MViT-16x4. However, for further investigation and understanding of MViT target model results, we re-assessed the results after adding MViT-32x3 as a source model. Figure 9 shows the results of MViT-16x4 target model after including MViT-32x3 source model. Figure 9a shows consistent results as shown in Figure 2a in which video understanding models are significantly better than image understanding ones. Figure 9b also shows consistent results to Figure 8a in which convolutional models are better than transformer-based models as predictors of MViT target model but with insignificant results, after adding MViT-32x3 source model to the transformers family, as anticipated.
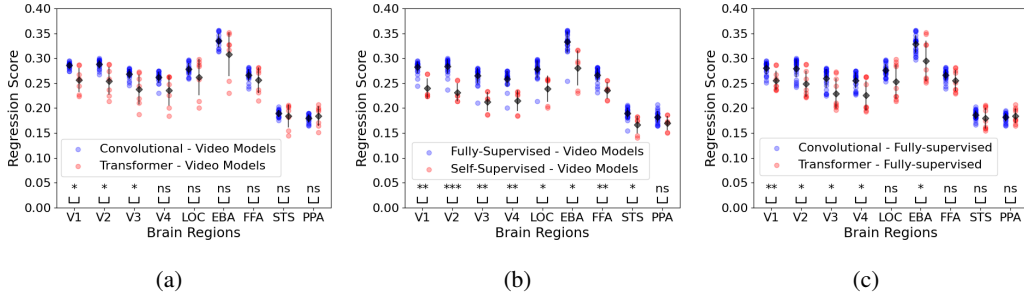
Figure 10: Real experiments showing regression scores as Pearson's correlation coefficient of model families on brain fMRI data with focus on video understanding models. (a) Comparison of convolutional *vs.* transformer-based amongst video understanding models. (b) Comparison of fully *vs.* self supervised amongst video understanding models. (c) Convolutional *vs.* transformer based fully-supervised models. Statistical significance is shown in the bottom as 'ns' not significant, '*, **, * * *' significant with p-values $< 0.05, 0.01, 0.001$, resp.
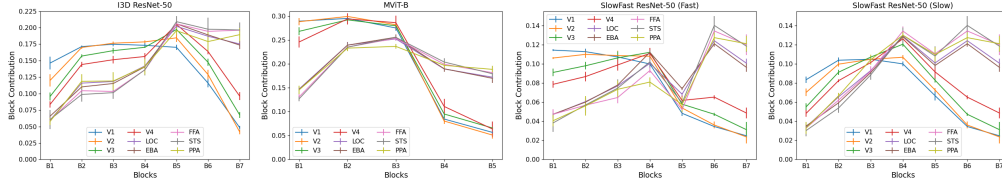

Figure 11: Layers contribution of four models for the nine regions of interest in the visual cortex.

B.3 ADDITIONAL REAL EXPERIMENTAL RESULTS

We add a study of the model subfamilies in terms of (a) convolutional *vs.* transformer based models and (b) fully *vs.* self supervised models, but focused on video understanding models only excluding models trained with single images. As shown in Fig. 10a it shows consistently that convolutional based models perform better in early layers as found earlier, where the first three regions show statistically significant results. Moreover, Fig. 10b shows models trained with self-supervision tend to be worse than fully supervised ones. However, note that these results are using a relatively small number of self-supervised learning video understanding models. Thus, we leave it for future work to expand on this further. Finally, we study the convolutional *vs.* transformer based models with focus on fully supervised ones excluding self supervision. Figure 10c shows the consistency of our results where the convolutional models in the early-mid regions surpass the transformer based ones.

B.4 ADDITIONAL FINE-GRAINED ANALYSIS

In this section, we provide additional fine-grained analysis for both real and simulated environments. First, we demonstrate the layer contribution of the studied video understanding models across different regions to have a better understanding of the hierarchical nature of biological neural systems. We show the layer contribution to the regression according to the regularized encoding technique in Section 3.3. Figure 11 shows the layer contribution for three video understanding models; MViT, I3D and SlowFast (Slow and Fast branches). It clearly demonstrates that across the four early layers in these networks, there is a higher contribution to the early and mid-level regions (V1-4), and the opposite occurs as we go deeper.

Second, in Fig. 12 we compare instances of convolutional (i.e., Slow) and transformer (i.e., TimeSformer) based models. It clearly shows that especially across the early-mid regions in the brain (i.e., V1-4), the convolutional models tend to provide better regression scores. This confirms our previous insight that convolutional models are better at capturing orientation and frequencies because of their early local connections. In later regions in the brain (i.e., LOC, EBA, FFA, STS, PPA) convolutional model (i.e., Slow) tends to act on-par or less than the transformer-based model (i.e., TimeSformer).
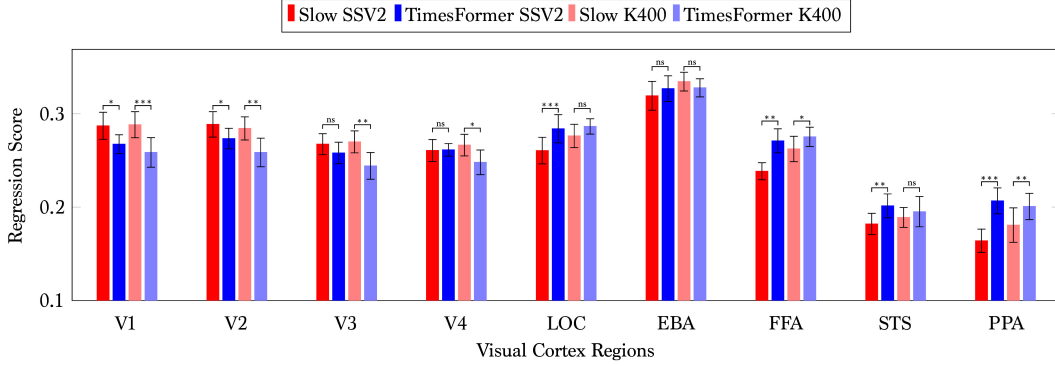
Figure 12: Fine-grained analysis comparing instances of Convolutional (i.e., Slow) *vs.* Transformer (i.e., TimeSformer) based models with different training datasets (SSv2 and K400).

Table 3: Fine-grained analysis of simulated experiments results in Fig. 2a with target model MViT-B 16x4 showing the worst (Min) and best (Max) source model from image & video understanding models. B1-5: Blocks in the target model.

	Min (Video)	Max (Video)	Min (Image)	Max (Image)
B1	OmniMAE-B-Fine	MViT-B-32x3	ResNet-34	ResNet-50
B2	OmniMAE-B-Fine	MViT-B-32x3	ViT-B-16	ResNet-152
B3	Slow-R50-SSv2	MViT-B-32x3	ViT-B-16	ResNet-101
B4	Slow-R50-SSv2	MViT-B-32x3	ViT-B-16	ResNet-34
B5	Slow-R50-SSv2	MViT-B-32x3	ViT-B-16	ResNet-101

Third, we analyze the best and worst across the models trained on single images *vs.* videos across both the simulated and real experiments. For the simulated experiments in Fig. 2, Table 3,4,5 and 6 show the worst (Min) and best (Max) predictors from each category (Image *vs.* Video) for target models MViT-B 16x4, ViT-B-16, ResNet-50, and I3D ResNet-50, respectively. For I3D, ResNet-50 and ViT, the results convey a simpler message that the best regressors are built with features extracted from architectures that exhibit higher similarity to the target model (i.e., convolutional/transformer) from both Video and Image understanding families. However, for MViT looking at Table 3 we see the best in the Image understanding models family is ResNet-50 which aligns with our previous insight that MViT tends to behave similar to convolutional models especially in the early layers.

Additionally, we show the best and worst predictors in the real experiments in Fig. 3 with the visual cortex regions as the target in Table 7. It shows both SlowFast and MViT are the best predictors from the video understanding family across the brain regions, with the SlowFast better at early regions similar to our previous findings as a two-stream and convolutional variant. It also shows ResNets to be the best from the image understanding family.

Fourth, we conduct an experiment comparing a randomly initialized network with respect to a trained model. The motivation behind this experiment is to confirm that our neural encoding is indeed capturing the learned representations in deep networks beyond random weights. Figure 13a shows SlowFast trained weights *vs.* random weights to confirm that the random weights provide worse correlation coefficient than the trained ones. This is indicative that our results are not only emergent from the architecture, but rather the learned representations that depend on architecture, dynamics encoding, training dataset and training signal (full/self supervision). Finally, we conduct experiments where we show the centered kernal alignment scores following previous works Han et al. (2023) in Fig. 13b. It shows that SlowFast, a video understanding model, surpasses ResNet-50, a single image understanding one, even when using another metric beyond the correlation coefficient of the regressed output.

Table 4: Fine-grained analysis of simulated experiments results in Fig. 2b with target model ViT-B-16 showing the worst (Min) and best (Max) source model from image & video understanding models. B1-4: Blocks in the target model.

	Min (Video)	Max (Video)	Min (Image)	Max (Image)
B1	MViT-B-32x3	OmniMAE-B-Fine	ResNet-101	ViT-L-16
B2	SlowFast-R50-Char	OmniMAE-B-Fine	ResNet-152	ViT-B-32
B3	SlowFast-R50-Char	OmniMAE-B-Fine	ResNet-34	ViT-L-16
B4	Slow-R50-SSv2	TimeSformer-K400	ResNet-18	ViT-B-32

Table 5: Fine-grained analysis of simulated experiments results in Fig. 2c with target model ResNet-50 showing the worst (Min) and best (Max) source model from image & video understanding models. B1-7: Blocks in the target model.

	Min (Video)	Max (Video)	Min (Image)	Max (Image)
B1	MViT-B-32x3	SlowFast-R50-SSv2	ViT-B-16	ResNet-34
B2	MViT-B-16x4	C2D	ViT-B-16	ResNet-152
B3	MViT-B-16x4	C2D	ViT-B-16	ResNet-18
B4	SlowFast-R50-Char	OmniMAE-B-Fine	ViT-B-16	ResNet-34
B5	SlowFast-R50-SSv2	TimeSformer-K400	ViT-B-16	ResNet-101
B6	Slow-R50-SSv2	TimeSformer-K400	ViT-B-16	ResNet-101
B7	Slow-R50-SSv2	TimeSformer-K400	ViT-B-16	ResNet-101

B.5 STATISTICAL SIGNIFICANCE RESULTS

Tables 8,9a shows the pairs of models from Fig. 4a (single-stream *vs.* two-stream) and Fig. 4b (fully-supervised *vs.* self-supervised) that exhibited a statistically significant result compared to each other. Table 8 confirms that two-stream models surpass the single-stream counterpart, across eight of the nine visual cortex regions, with a statistically significant result. The table specifically shows that the superiority of the two-stream models is independent of the training dataset. In five of nine brain regions, the two-stream models were superior compared to single-stream models at two different model versions that were matched based on their training dataset (K400 and Charades). On the other hand, Table 9a confirms that fully-supervised (i.e., OmniMAE Fine and TimeSformer) surpass the self-supervised counterpart (i.e., OmniMAE Pre) across all the visual cortex regions with a statistically significant result when the three models share the same architecture base (ViT-B) and training dataset (SSv2). These results, in addition to Fig. 4b, show that TimeSformer (trained solely using full-supervision) achieved the highest regression scores followed by OmniMAE Fine (trained using both self- and full-supervision) and finally OmniMAE Pre (trained solely using self-supervision). It demonstrates that full-supervision better reflects the visual cortex responses. Table 9b shows the significance results between video understanding pairs of models. As shown in Table 9b and Fig. 4c, SlowFast is statistically better than I3D in seven of the nine brain regions, I3D is statistically better than stMAE in five brain regions including four early regions of the visual cortex (V1 to V4), while SlowFast is not statistically different than MViT in any of the regions.

B.6 ADDITIONAL RESULTS ON INTER-INTRA REGION CONNECTIVITY

In this section, we provide additional ablations on the connectivity module. We compare our learned connectivity to a simple random or an identity connectivity in Tables 10 and 11. In the random connectivity model, we assign random weights (using Xavier initialization) to the fully-connected layers in the connectivity model. On the other hand, in the identity connectivity model, we assign identity weights (ones) to the fully-connected layers. The connectivity model with identity weights represents a model where each region is learning from all the regions equally. The results clearly show that our learned connectivity surpasses these lower baselines of random or identity initialized connectivity.

Table 6: Fine-grained analysis of simulated experiments results in Fig. 2d with target model I3D ResNet-50 showing the worst (Min) and best (Max) source model from image & video understanding models. B1-7: Blocks in the target model.

	Min (Video)	Max (Video)	Min (Image)	Max (Image)
B1	MViT-B-32x3	CSN	ViT-B-16	ResNet-34
B2	MViT-B-16x4	SlowFast-R101	ViT-B-16	ResNet-18
B3	MViT-B-32x3	C2D	ViT-B-16	ResNet-18
B4	MViT-B-32x3	C2D	ViT-L-32	ResNet-18
B5	OmniMAE-B-Fine	X3D-L	ViT-B-16	ResNet-50
B6	SlowFast-R50-SSv2	C2D	ViT-B-16	ResNet-101
B7	Slow-R50-SSv2	SlowFast-R50-K400	ViT-B-16	ResNet-101

Table 7: Fine-grained analysis of real experiments results in Fig. 3a with target model the visual cortex regions showing the worst (Min) and best (Max) source model from image & video understanding models.

	Min (Video)	Max (Video)	Min (Image)	Max (Image)
V1	stMAE	SlowFast-R50-8x8-Char	MAE	ResNet-18
V2	OmniMAE-B-Pre	SlowFast-R50-8x8-Char	MAE	ResNet-50
V3	OmniMAE-B-Pre	SlowFast-R50-8x8-K400	MAE	ResNet-50
V4	OmniMAE-B-Pre	SlowFast-R101	ViT-L-32	ResNet-50
LOC	OmniMAE-B-Pre	MViT-B-32x3	ViT-B-16	ResNet-101
EBA	OmniMAE-B-Pre	SlowFast-R101	ViT-B-16	ResNet-101
FFA	OmniMAE-B-Pre	SlowFast-R50-8x8-Char	ViT-B-16	ResNet-101
STS	OmniMAE-B-Pre	MViT-B-32x3	ViT-B-16	ResNet-101
PPA	OmniMAE-B-Pre	TimeSformer-SSv2	ViT-B-16	ResNet-50

B.7 COMPARISON TO STATE-OF-THE-ART METHODS ON ALGONAUTS BENCHMARK

This work focuses on studying video understanding models from a neuroscience perspective through a large-scale comparison of state-of-the-art deep video understanding models to the visual cortex recordings. Additionally, we propose a novel encoding approach using inter-intra region connectivity on the top of pre-trained deep neural network models to predict visual cortex voxel activity. To study the effect of our novel encoding approach, we compared the accuracy achieved by our best model (MViT-B with connectivity priors) to the state-of-the-art (SOA) accuracies achieved per region Zhou et al. (2022). In Zhou et al. (2022), they similarly built their encoding models on pre-trained deep learning models using the layer-weighting approach and their best model varied per brain region. Accordingly, we compare our best model results with their best model per region as shown in figure 14. It shows that our novel encoding approach achieved on average higher results across all the regions except for PPA in which it is on par. This comparison shows the accuracy enhancement achieved compared to the state of the art by incorporating connectivity priors to features extracted from pre-trained deep learning models. Note that our approach has a stronger form of cross validation as we take the mean of different subjects and we compute statistics across four folds from different videos. As such, our comparison to the baseline with no connectivity that follows Zhou et al. (2022) in Fig. 5a, better reflects our improvement gains. In future work, we will further explore the effect of integrating connectivity priors with end-to-end fine-tuning of deep learning models and ensemble approaches.

C LIMITATIONS

In this section, we discuss limitations of our work. Our current large-scale study is limited to ten subjects watching short video clips with 1,000 videos provided. We leave it for future work to explore the collection of broader datasets with longer videos up to 5-10 minutes towards the creation of foundation models for neural encoding.
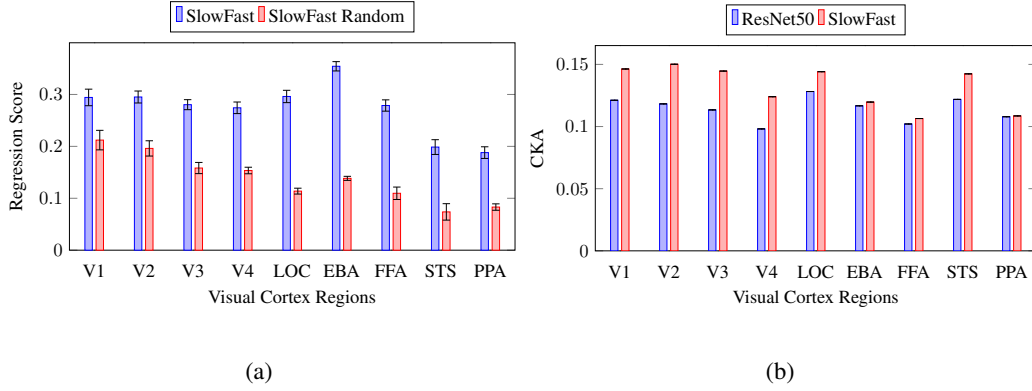
Figure 13: (a) Comparison between a trained and randomized SlowFast model. (b) Centered Kernal Alignment (CKA) for ResNet50 and SlowFast models. It shows the consistency of our results using other metrics beyond the regression score.

Table 8: Statistical Significant of Slow *vs.* SlowFast (Fig. 4a, showing the pairs of models (.,.) that exhibited statistical significance. K400: Kinetics 400, Char: Charades that were used as training datasets.

	Stat. Sig.
V1	SlowFast-Char, Slow-Char
V2	SlowFast-K400, Slow-K400 SlowFast-Char, Slow-Char
V3	SlowFast-K400, Slow-K400 SlowFast-Char, Slow-Char
V4	SlowFast-K400, Slow-K400
LOC	SlowFast-K400, Slow-K400 SlowFast-Char, Slow-Char
EBA	SlowFast-K400, Slow-K400 SlowFast-Char, Slow-Char
FFA	SlowFast-K400, Slow-K400 SlowFast-Char, Slow-Char
STS	SlowFast-K400, Slow-K400

D BROADER IMPACT

Conducting large-scale study on neural encoding of biological neural systems in comparison to deep neural networks, has multiple positive societal impacts as it can be used to drive insights into the understanding and advancement of deep networks. Our study also improved our understanding of the human visual cortex and its connectivity using our learned inter-intra region connectivity model, which is useful in various applications. Applications for neural encoding have various benefits including providing a way for testing and understanding brain mechanisms and computations in addition to multiple neural interfaces applications. Since the neural encoding modelling and its capabilities is still being developed and relatively in its infancy, in addition to the datasets available being limited in size, we do not perceive any negative societal impact from such developed models.

Table 9: (a) Statistical Significant of Self-supervised *vs.* Fully Supervised (Fig. 4b), showing the pairs of models (.,.) that exhibited statistical significance. (b) Statistical Significant of video understanding models (Fig. 4c), showing pairs of models (.,.) that exhibited statistical significance.

(a)

	Stat. Sig.
V1	OmniMAE Pre, OmniMAE Fine OmniMAE Pre, TimeSformer
V2	OmniMAE Pre, OmniMAE Fine OmniMAE Pre, TimeSformer
V3	OmniMAE Pre, OmniMAE Fine OmniMAE Pre, TimeSformer
V4	OmniMAE Pre, OmniMAE Fine OmniMAE Pre, TimeSformer
LOC	OmniMAE Pre, TimeSformer
EBA	OmniMAE Pre, TimeSformer
FFA	OmniMAE Pre, TimeSformer
STS	OmniMAE Pre, TimeSformer
PPA	OmniMAE Pre, OmniMAE Fine OmniMAE Pre, TimeSformer

(b)

	Stat. Sig.
V1	SlowFast-R50-8x8, I3D stMAE, I3D
V2	SlowFast-R50-8x8, I3D stMAE, I3D
V3	SlowFast-R50-8x8, I3D stMAE, I3D
V4	SlowFast-R50-8x8, I3D stMAE, I3D
LOC	SlowFast-R50-8x8, I3D stMAE, I3D
EBA	SlowFast-R50-8x8, I3D
PPA	SlowFast-R50-8x8, I3D

Table 10: MViT learnable connectivity results compared to the base model without connectivity and other lower baselines, i.e., random and identity connectivity.

Regions	Base Model	Learnable Connectivity	Random Connectivity	Identity Connectivity
V1	0.287	0.297	-0.001	0.090
V2	0.288	0.299	0.001	0.109
V3	0.270	0.283	0.000	0.121
V4	0.263	0.272	0.000	0.108
LOC	0.293	0.316	0.000	0.163
EBA	0.349	0.369	0.000	0.223
FFA	0.281	0.306	0.002	0.164
STS	0.204	0.232	0.001	0.108
PPA	0.194	0.218	-0.002	-0.009

E ASSETS AND LICENCES

We use the Mini-Algonauts Project 2021 Cichy et al. (2021) dataset that was provided in the challenge and its development kit which is licensed under a MIT License that allows its use without restriction. The Bold Moments Dataset (BMD) including the fMRI data and stimulus metadata we used in this study is available in the OpenNeuro database under accession code DS005165 and CC0 License Lahner et al. (2024). Most of our image and video understanding models and their trained weights are used from Pytorch Paszke et al. (2019) and Pytorch Video Fan et al. (2021a), except for few models that were retrieved from their publicly released codes and model weights.

Table 11: SlowFast learnable connectivity results compared to the base model without connectivity and other lower baselines, i.e., random and identity connectivity.

Regions	Base Model	Learnable Connectivity	Random Connectivity	Identity Connectivity
V1	0.294	0.301	0.001	0.101
V2	0.295	0.305	-0.001	0.121
V3	0.280	0.288	-0.001	0.129
V4	0.274	0.285	-0.002	0.127
LOC	0.296	0.311	-0.001	0.156
EBA	0.354	0.360	-0.001	0.218
FFA	0.279	0.293	-0.004	0.153
STS	0.199	0.227	0.002	0.097
PPA	0.188	0.204	0.000	-0.019
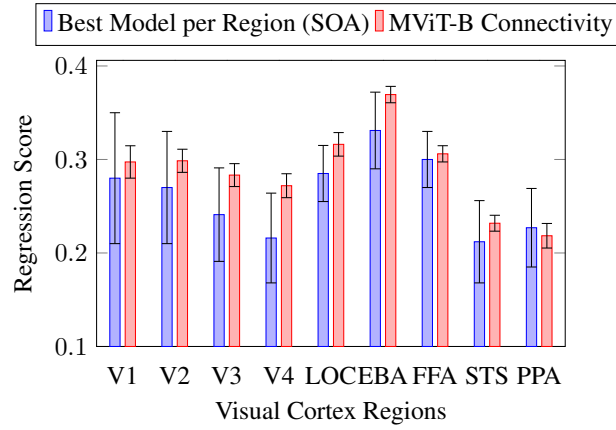
(a)

Figure 14: Comparison of MViT-B with connectivity priors to the state-of-the-art model per region as presented in Zhou et al. (2022).